J Fluoresc (2010) 20:381–387
DOI 10.1007/s10895-009-0543-2

SHORT COMMUNICATION

Spectroscopic Investigation on the Toxicological Interactions of 4-aminoantipyrine with Bovine Hemoglobin

Yue Teng · Rutao Liu · Shifeng Yan · Xingren Pan · Pengjun Zhang · Meijie Wang

Received: 22 July 2009 / Accepted: 15 September 2009 / Published online: 29 September 2009

Abstract The effects of 4-aminoantipyrine (AAP) on bovine hemoglobin (BHb) were investigated by fluorescence spectroscopy, synchronous fluorescence spectroscopy, ultraviolet-visible absorption spectroscopy and circular dichroism spectroscopy (CD) under simulated physiological conditions. The experimental results showed that AAP effectively quenched the intrinsic fluorescence of BHb via static quenching. The number of binding sites, the binding constant K_a, and the thermodynamic parameters (ΔH°, ΔS° and ΔG°) were measured at two different temperatures. Van der Waals' interactions and hydrogen bonds were the predominant intermolecular forces in stabilizing the BHb-AAP complex. The experiment results confirmed micro-environmental and conformational changes of BHb in the presence of AAP. The α-helix content decreased, indicating that AAP destroys some of the hydrogen bonding networks in the polypeptide chain.

Keywords 4-aminoantipyrine · Bovine hemoglobin · Multi-spectroscopic techniques · Toxicity evaluation

Electronic supplementary material The online version of this article (doi:10.1007/s10895-009-0543-2) contains supplementary material, which is available to authorized users.

Y. Teng · R. Liu (✉) · X. Pan · P. Zhang · M. Wang
Shandong Key Laboratory of Water Pollution Control and Resource Reuse, School of Environmental Science and Engineering, Shandong University,
27 Shanda South Road,
Jinan 250100, People's Republic of China
e-mail: rutaoliu@sdu.edu.cn

S. Yan
College of Science, Qingdao Agricultural University,
Qingdao 266109, People's Republic of China

Introduction

4-Aminoantipyrine (AAP, in support information Fig. 1) is a metabolite of aminophenazone and is an aromatic substance with analgesic, anti-inflammatory and antipyretic properties. Although today AAP is scarcely administered as analgesic because of the risk of agranulocytosis [1], it is mostly used as a reagent for biochemical reactions producing peroxides or phenols [2, 3] and is also be used to detecting phenols in environment [4]. Due to AAP is widely used in biochemical experiment and in environmental monitoring, AAP as an aromatic pollutant exposes in the environment.

Hemoglobin is the iron-containing oxygen-transport metalloprotein in the red blood cells. As a carrier of oxygen, hemoglobin transports oxygen from the lungs or gills to the rest of the body where it releases the oxygen for cell use. It is also responsible for the maintenance of blood pH [5, 6]. Hemoglobin has four subunits, composed of two α-chains and β-chains. Thus, the subunit structure of hemoglobin is $\alpha_2\beta_2$ [7]. The α-chains contain 141 amino acids; the β-chains contain 146 amino acids. The four subunits are held together at their contacting sites by hydrophobic bonds and salt bridges [8, 9]. Many factors can impact the normal physiological functions of hemoglobin. Not only endogenous physiological conditions (pH, temperature, etc), but also exogenous environmental pollutants (heavy metals, organic pollutants, etc) can impact protein conformation and function. Hemoglobin is involved in many diseases such as leukemia, anemia and heart disease [10, 11]. Research on the molecular mechanisms of toxicity of environmental contaminants and methods to evaluate the toxicity of aromatic organic compounds are at the forefront of environmental toxicology today [12, 13].

The toxic effect of 4-aminoantipyrine on experimental animals has been reported [14]. AAP can reduce blood flow [15] and 13,14-dihydro-15-keto prostaglandin F2 alpha concentration [16] after it infused into the blood. AAP can form stable complexes with heme [17], but little work has been focused on the molecular interactions of AAP with the functional protein of hemoglobin. In this work, we investigated the interaction mechanisms of AAP with bovine hemoglobin (BHb) by fluorescence spectroscopy, synchronous fluorescence spectroscopy, ultraviolet-visible absorption spectroscopy and circular dichroism spectroscopy (CD). We determined the binding constants and the thermodynamic parameters. The effect of 4-aminoantipyrine on the conformation of BHb was also investigated, which would inevitably affect its normal function, and thereby induce the potential threat of toxicity to the body.

Experimental

Reagents

Bovine hemoglobin (BHb) was obtained from Beijing Biodee Biotechnology Co., Ltd. 4-aminoantipyrine was obtained from Tianjin Chemical Reagent Co., Ltd. AAP was dissolved with ultra-pure water as a stock solution, 1.0×10^{-3} molL^{-1}. Tris-hydroxymethyl-methane (Tris) was purchased from Sinopharm Chemical Reagent Co., Ltd. HCl and NaCl were all of analytical reagent grade. Physiological buffer (Tris-saline buffer) was 0.05 molL^{-1} Tris-HCl with 0.15 molL^{-1} NaCl, pH 7.4. All solutions were prepared with ultra-pure water (18.25 MΩ).

Apparatus and measurements

All fluorescence spectra were recorded on F-4600 fluorescence spectrophotometer (Hitachi Japan) in a 1-cm cell. The excitation wavelength was 280 nm. The excitation and emission slit widths were set at 5 nm. Scan speed was 1200 nm/min. PMT (Photo Multiplier Tube) voltage was 700 V.

Synchronous fluorescence spectra of BHb in the absence and presence of 4-aminoantipyrine were measured ($\Delta\lambda$= 15 nm, λ_{ex}=270–320 nm and $\Delta\lambda$=60 nm, λ_{ex}=250–320 nm, respectively). The excitation and emission slit widths were set at 5 nm. Scan speed was 1200 nm/min. PMT voltage was fixed at 700 V.

The absorption spectra were recorded on a double beam UV-2450 spectrophotometer (Shimadzu, Japan) equipped with 1.0-cm quartz cells. Slit width was set at 2.0 nm. The wavelength range was 500–200 nm.

Circular dichroism (CD) measurements were made on a J-810 Spectropolarimeter (Jasco, Tokyo, Japan) in a 1-cm cell at room temperature. Bandwidth was 1 nm and scanning speed was 200 nm/min.

Results and discussion

Fluorescence measurements

BHb can emit intrinsic fluorescence mainly due to Trp and Tyr residues. BHb contains six Trp residues in $\alpha_2\beta_2$ tetramer: two α-14 Trp, two β-15 Trp and β-37 Trp [18]. Of the three Trp residues, only the β-37 Trp is located in the internal hydrophobic region of BHb and plays a key role in the intrinsic fluorescence of BHb. BHb contains five Tyr residues in each αβ dimer: α-Tyr 24, 42, 140 and β-Tyr 34, 144, but the fluorescence intensity of Tyr is much smaller than that of Trp. Changes of emission spectra can provide information about their structure and dynamics. Fluorescence emission spectra of BHb with different AAP concentrations at room temperature were recorded (Fig. 1). It can be seen from Fig. 1 that the fluorescence intensity decreased with the increasing concentration of AAP. The fluorescence quenching of BHb by AAP indicated that AAP can bind to BHb and alter the structure of BHb.

The fluorescence quenching mechanism

Since AAP can quench the intrinsic fluorescence of BHb, we further analyzed the quenching mechanism. Quenching mechanisms are usually classified into dynamic and static

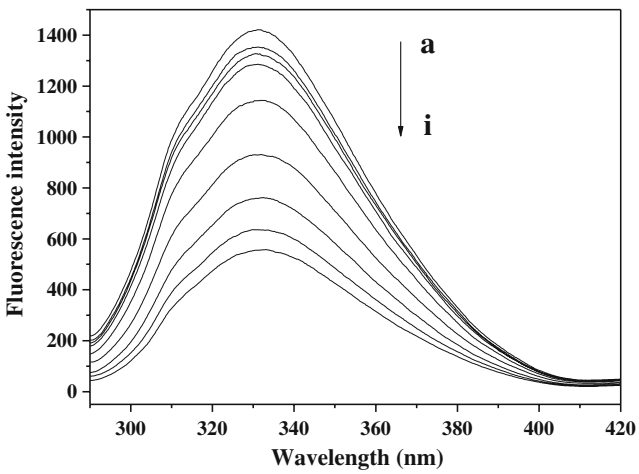

Fig. 1 The influence of AAP on the fluorescence emission spectra of BHb. Conditions: BHb 3.0×10^{-6}molL^{-1}; AAP **a** 0, **b** 3×10^{-6}, **c** 6×10^{-6}, **d** 1×10^{-5}, **e** 2×10^{-5}, **f** 4×10^{-5}, **g** 6×10^{-5}molL^{-1}, **h** 8×10^{-5} molL^{-1}, **i** 1×10^{-4}molL^{-1}; Tris-HCl 0.05 molL^{-1} (pH=7.4); NaCl 0.15 molL^{-1}

quenching. Since higher temperature results in larger diffusion coefficients, the dynamic quenching constants will increase with increasing temperature. In contrast, increased temperature is likely to result in decreased stability of complexes, and thus the static quenching constants are expected to decrease with increasing temperature [19]. In order to confirm the quenching mechanism of the interaction of AAP and BHb, we analyzed the fluorescence spectra at different temperatures with the well-known Stern-Volmer equation:

$$\frac{F_0}{F} = 1 + Ksv[Q] = 1 + k_q\tau_0[Q] \quad (1)$$

where F_0 and F are the fluorescence intensity in the absence and presence of the quencher, [Q] is the concentration of the quencher, τ_0 is the fluorescence lifetime in the absence of quencher, and k_q is the quenching rate constant of the biological macromolecule. K_{SV} is the Stern-Volmer quenching constant.

Fluorescence intensity data were analyzed according to F_0/F versus [Q] at 294 K and 308 K (Fig. 2). Eq. (1) was applied to determine K_{SV} (Table 1) by a linear regression plot of F_0/F against [Q]. The value of K_q was also obtained (the fluorescence lifetime of the biopolymer (τ_0) is 10^{-8}s [20]).

Since the maximum scatter collision quenching constant of various quenchers with a biopolymer is usually 2.0×10^{10}Lmol^{-1}s^{-1} [21], the values of K_q at 294 and 308 K were far greater than 2.0×10^{10} Lmol^{-1}s^{-1}. Furthermore, the K_{SV} values (Table 1) decreased with higher temperature. Thus, the results indicated that the overall quenching is dominated by a static quenching mechanism forming an AAP-BHb complex.

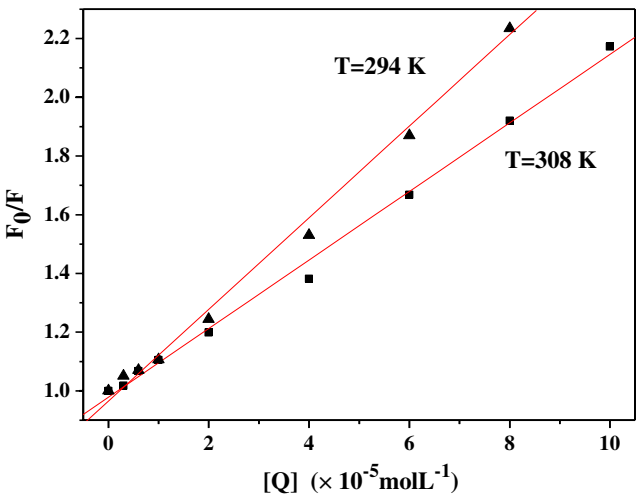

Fig. 2 Stern-Volmer plots for the quenching of BHb by AAP at 294 K and 308 K

Binding constant and binding capacity

From the above results, we determined that the fluorescence quenching mechanism was a static quenching. The quenching came from formation of a complex between BHb and AAP. Then, fluorescence intensity data can also be used to obtain the binding constant (K_a) and the number of binding sites (n) for a small molecular-protein complex [22]. The relationship between the fluorescence intensity and the quenching medium can be deduced from the formula:

$$\lg\frac{(F_0 - F)}{F} = \lg Ka + n\lg[Q] \quad (2)$$

where F_0, F and [Q] are the same as in Eq. (1), K_a is the binding constant and n is the number of binding sites. The values of n and K_a (Table 2) were calculated and the number of binding sites is about 1.127 (approximately equal to 1). It can be concluded that there is one binding site of AAP to BHb. The value of K_a is 4.95×10^4Lmol^{-1} in room temperature. The value of K_a as obtained is of the order of 10^4, indicating that a strong interaction exists between AAP and BHb. Even if a low concentration of AAP is present in the blood, AAP can interact with BHb easily.

Determination of the interaction forces between AAP and BHb

Small molecules can bind to biological macromolecules through four binding modes: hydrogen bonds, hydrophobic forces, electrostatic forces and van der Waals' interactions. The noncovalent interaction forces between proteins and small molecules can be determined by thermodynamic parameters. If $\Delta H^\circ\approx0$, $\Delta S^\circ>0$, hydrophobic interaction plays a major role in the reaction; if $\Delta H^\circ<0$, $\Delta S^\circ>0$, the main force is electrostatic effect; if $\Delta H^\circ<0$, $\Delta S^\circ<0$, the main forces are van der Waals and hydrogen bond interactions [23].

When the change of temperature is small, ΔH° can be considered a constant, and can be approximated from Eq. (3). The free-energy change (ΔG°) and the entropy change (ΔS°) of the binding reaction follow Eqs. (4) and (5), respectively.

$$\ln\left(\frac{K_2}{K_1}\right) = \left(\frac{1}{T_1} - \frac{1}{T_2}\right)\left(\frac{\Delta H^\circ}{R}\right) \quad (3)$$

$$\Delta G^\circ = -RT\ln K^\circ \quad (4)$$

$$\Delta G^\circ = \Delta H^\circ - T\Delta S^\circ \quad (5)$$

where K_1 and K_2 are the binding constants (analogous to K_a in Eq. (2)) at T_1 and T_2, and R is the universal gas constant.

Table 1 Stern-Volmer quenching constants for the interaction of AAP with BHb at 294 K and 308 K

pH	T (K)	K_{SV} ($\times 10^5 Lmol^{-1}$)	k_q ($\times 10^{12} Lmol^{-1}s^{-1}$)	R[a]	S.D.[b]
7.4	294	1.56	15.6	0.9981	0.0381
	308	1.17	11.7	0.9980	0.0294

[a] R is the correlation coefficient

[b] S.D. is the standard deviation for the K_{SV} values

The values of the thermodynamic parameters were $\Delta H^\circ = -70.56\ kJmol^{-1}$, $\Delta G^\circ = -26.4\ kJmol^{-1}$ and $\Delta S^\circ = -150.2\ Jmol^{-1}K^{-1}$ at ambient temperature (shown in Table 2). Negative ΔG° means that the interaction process was spontaneous and the negative ΔH° and negative ΔS° indicate that van der Waals forces and hydrogen bonds play the major roles in the protein-AAP interaction.

Conformational investigations

Since spectroscopy allows non-intrusive measurement of substances, it is a useful tool to investigate conformational changes of proteins, even at the low concentrations that are typical of physiological conditions [23, 24]. In this work, synchronous fluorescence, UV-vis absorption and circular dichroism spectroscopy were used to evaluate the conformational changes of BHb.

Synchronous fluorescence spectroscopy

Synchronous fluorescence spectroscopy is a common method for the evaluation of protein conformational changes and it involves simultaneous scanning of the excitation and emission monochromators while maintaining a constant wavelength interval between them. Synchronous fluorescence spectroscopy can give information about the molecular environment in the vicinity of a chromophore such as tryptophan and tyrosine. The shift in the emission maximum (λ_{em}) reflects the changes of polarity around the chromophore molecule [25]. When the $\Delta\lambda$ between excitation and emission wavelength is set at 15 nm, the synchronous fluorescence gives characteristic information of tyrosine residues. And when $\Delta\lambda$ is fixed at 60 nm, a spectrum characteristic of tryptophan residues is obtained [26, 27]. The synchronous fluorescence spectra at these two different wavelength intervals are presented in Fig. 3.

As the concentration of AAP increased gradually, the synchronous fluorescence intensity decreased and an obvious red shift of the tyrosine peak in Fig. 3a could be observed, which indicates that the hydrophobicity of the tyrosine residues decreased and the tyrosines buried in the nonpolar hydrophobic cavities were moved to a more hydrophilic environment. In Fig. 3b, the maximum emission wavelength of tryptophan kept its position over the investigated concentration range. We concluded that there was no change in the microenvironment of the tryptophan residues. It is apparent in Fig. 4 that the slope was higher when $\Delta\lambda$ was 15 nm indicating AAP was closer to the tyrosine residues than to the trytophan residues. Indeed, the microenvironment of the tryptophan residues was not altered by AAP and tyrosine was moved to a more hydrophilic environment.

UV-vis absorption spectroscopy

UV-vis absorption can be applied to explore protein structural changes and to investigate protein-ligand complex formation. We recorded the UV-vis absorption spectra of the AAP, BHb and AAP-BHb system (Fig. 5). UV-vis absorption spectra of BHb in the absence and presence of AAP were obtained by using the corresponding concentration of AAP in free form as the reference solution. The absorption peak of BHb at about 210 nm reflects the framework conformation of the protein [23, 28, 29]. At very low concentrations AAP did not affect the absorption spectra of BHb. As the concentration of AAP increased, the absorbance of BHb decreased and the maximum peak position of BHb-AAP was red shifted, which indicates an interaction between AAP and BHb. The absorbance shift

Table 2 Binding constants K_a and relative thermodynamic parameters of the AAP-BHb system

T (K)	K_a ($\times 10^4 Lmol^{-1}$)	n	R[a]	ΔH° ($kJmol^{-1}$)	ΔS° ($Jmol^{-1}K^{-1}$)	ΔG° ($kJmol^{-1}$)
294	4.95	1.127	0.9990	−70.56	−150.2	−26.4
308	1.35	1.022	0.9979		−149.9	−24.4

[a] R is the correlation coefficient for the K_a values

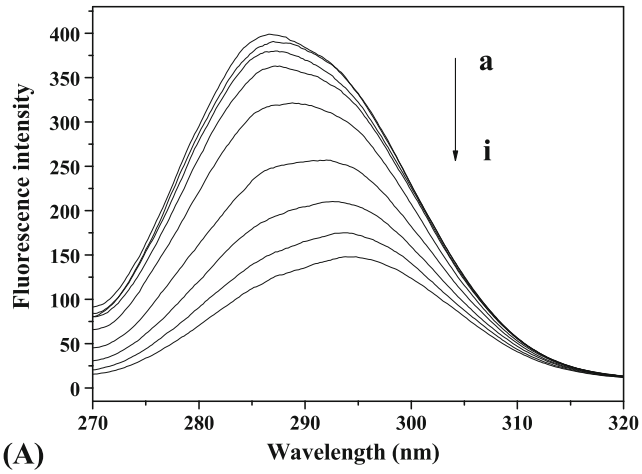

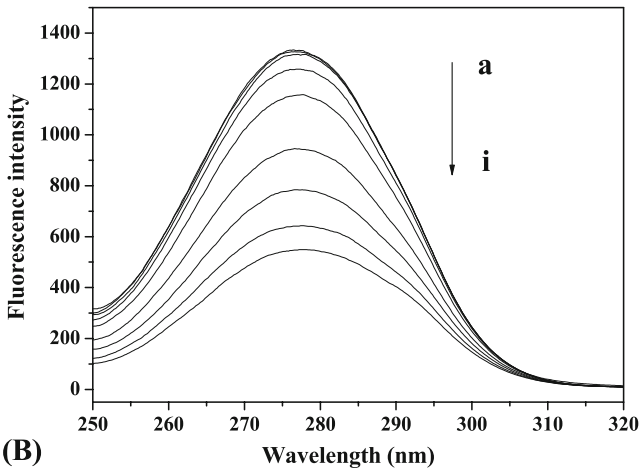

Fig. 3 Synchronous fluorescence spectra of BHb. Conditions: **a** Δλ= 15 nm and **b** Δλ=60 nm. BHb 3.0×10^{-6}molL^{-1}; AAP (a–i): 0, 3×10^{-6}, 6×10^{-6}, 1×10^{-5}, 2×10^{-5}, 4×10^{-5}, 6×10^{-5}, 8×10^{-5}, 1×10^{-4} molL^{-1}; Tris-HCl 0.05 molL^{-1} (pH=7.4); NaCl 0.15 molL^{-1}

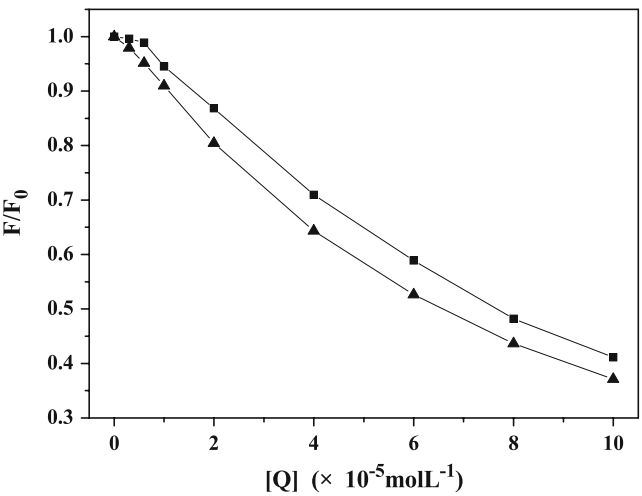

Fig. 4 The quenching of BHb synchronous fluorescence by AAP. Conditions: BHb 3.0×10^{-6} molL^{-1}. (▲) Δλ=15 nm and (■) Δλ= 60 nm

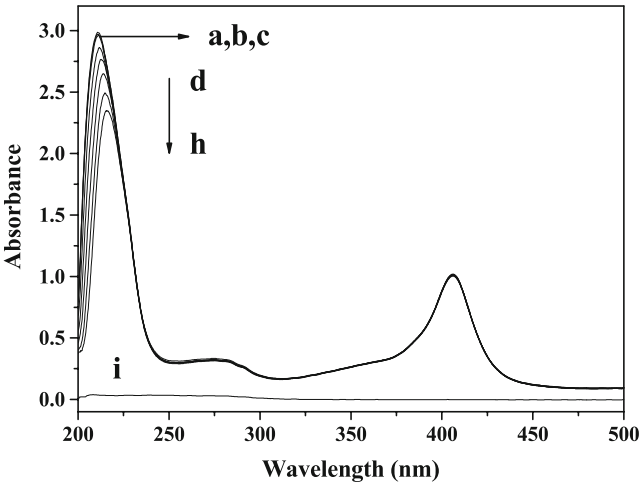

Fig. 5 Absorption spectra of AAP, BHb and BHb-AAP. Conditions: BHb concentration (**a**–**h**) was fixed at 3×10^{-6}molL^{-1}; AAP concentrations in AAP-BHh system (**a**–**h**) were 0, 3×10^{-6}, 1×10^{-5}, 4×10^{-5}, 6×10^{-5}, 8×10^{-5}, 1.2×10^{-4}, 1.6×10^{-4}, 2×10^{-4}molL^{-1}; AAP concentration (**i**) was 1×10^{-5}molL^{-1}. AAP of the same concentration was used as the reference solution (**a**–**h**)

indicates that the hydrophobicity was decreased and the peptide strands of BHb became more extended [30], therefore the binding between AAP and BHb leads to changes in the BHb conformation.

Circular dichroism spectroscopy

CD is a sensitive technique to monitor the conformational changes of proteins upon interaction with small molecules. The CD spectra of BHb in the absence and presence of AAP are shown in Fig. 6. The CD spectra of BHb exhibited two negative bands in the ultraviolet region at 208 and 222 nm, which is characteristic of the α-helix of proteins

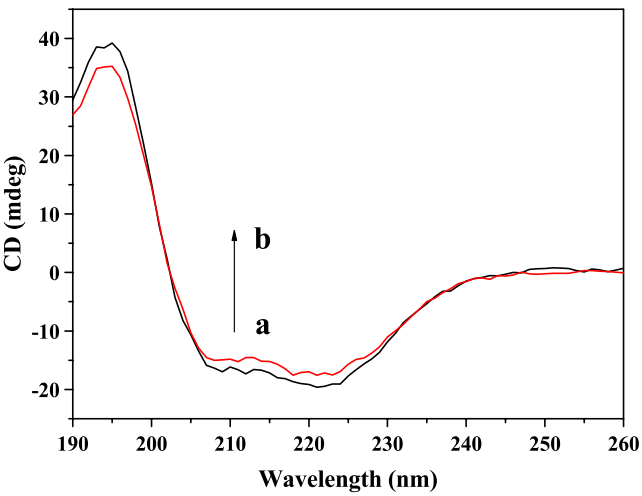

Fig. 6 CD spectra of the AAP-BHb system at room temperature. Conditions: **a** BHb 2.0×10^{-7}molL^{-1}; **b** BHb 2.0×10^{-7}molL^{-1} + AAP 2×10^{-6}molL^{-1}

[23]. The α-helical content of BHb in the absence and presence of AAP were calculated from Eq. (6) and Eq. (7).

$$MRE = \frac{ObservedCD(m\,\deg)}{C_p nl \times 10} \tag{6}$$

where C_P is the molar concentration of the protein, n is the number of amino acid residues and l is the path length.

$$\alpha - Helix(\%) = \frac{-\mathrm{MRE}_{208} - 4000}{33,000 - 4000} \times 100 \tag{7}$$

where MRE_{208} is the observed MRE (mean residual ellipticity) at 208 nm, 4000 is the MRE of the β-form and random coil conformation cross at 208 nm, and 33,000 is the MRE value of a pure α-helix at 208 nm. From the above equations, quantitative analysis results for the amount of α-helix in the secondary structure of BHb were obtained. The α-helicity decreased from 35.3% in free BHb to 31.3% in the BHb-AAP system. The decrease of α-helix content indicates that AAP combines with the amino acid residues of the main polypeptide chain of the protein and destroys their hydrogen bond networks [23, 31]. So, we conclude that the binding of AAP to BHb induces conformational changes in BHb and that AAP has an obvious denaturing effect on BHb.

Conclusions

In this paper, the interaction of AAP and BHb was investigated by multiple spectroscopic techniques including fluorescence spectra, synchronous fluorescence spectra, UV-vis absorption spectra and CD spectra. AAP effectively quenched the fluorescence of BHb by a static quenching process. There was a strong interaction between AAP and BHb with approximately one binding site. The thermodynamic parameters ΔH°, ΔS° and ΔG° were also calculated. The negative values of enthalpy change ΔH° and entropy change ΔS° indicated that van der Waals interactions and hydrogen bonds played a major role in stabilizing the complex. Based on the results of synchronous fluorescence spectra, UV-vis absorption spectra and CD spectra, the microenvironment and conformation of BHb was demonstrably changed in the presence of AAP. The skeletal structure of BHb loosened, exposing internal hydrophobic aromatic ring amino acids and peptide strands to the solution. All these experimental results and theoretical data reveal that AAP has an obvious denaturing effect on BHb.

Acknowledgments We gratefully acknowledge the financial support of Natural Science Foundation of China (20607011, 20875055), the Cultivation Fund of the Key Scientific and Technical Innovation Project, Ministry of Education of China (708058), NCET-06-0582, Fok Ying Tong Education Foundation (111082), Foundation for Excellent Young Scientists and Key Science-Technology Project in Shandong Province (2007BS08005, 2008GG10006012). The authors thank Dr. Pamela Holt for editing this manuscript.

References

1. Lang A, Hatscher C, Wiegert C, Kuhl P (2009) Protease-catalysed coupling of N-protected amino acids and peptides with 4-aminoantipyrine. Amino Acids 36(2):333–340
2. Van Staden JF, Beyene NW, Stefan RI, Aboul-Enein HY (2005) Sequential injection spectrophotometric determination of ritodrine hydrochloride using 4-aminoantipyrine. Talanta 68(2):401–405
3. Kasthuri J, Santhanalakshmi J, Rajendiran N (2008) Platinum nanoparticle catalysed coupling of phenol derivatives with 4-aminoantipyrine in aqueous medium. Transit Metal Chem 33 (7):899–905
4. Katsaounos CZ, Paleologos EK, Giokas DL, Karayannis MI (2003) The 4-aminoantipyrine method revisited: Determination of trace phenols by micellar assisted preconcentration. Int J Environ An Ch 83(6):507–517
5. Munoz G, Juan AD (2006) PH— and time-dependent hemoglobin transitions: A case study for process modelling, 10th International Conference on Chemometrics in Analytical Chemistry. Elsevier Science Bv, Aguas de Lindoia, BRAZIL, p198–208
6. Zheng CY, Ma GH, Su ZG (2007) The role of pH and its control on effective conjugation of bovine hemoglobin and human serum albumin. Process Biochem 42(3):303–309
7. Hirsch RE, Zukin RS, Nagel RL (1980) Intrinsic fluorescence emission of intact oxy hemoglobins. Biochem Biophys Res Commun 93(2):432–439
8. Nichols WL, Zimm BH, Ten Eyck LF (1997) Conformation-invariant structures of the alpha1beta1 human hemoglobin dimer. J Mol Biol 270(4):598–615
9. Li R, Nagai Y, Nagai M (2000) Changes of tyrosine and tryptophan residues in human hemoglobin by oxygen binding: near— and far-UV circular dichroism of isolated chains and recombined hemoglobin. J Inorg Biochem 82(1–4):93–101
10. Reeder BJ, Wilson MT (2005) Hemoglobin and myoglobin associated oxidative stress: From molecular mechanisms to disease states. Curr Med Chem 12(23):2741–2751
11. Wajcman H, Traeger-Synodinos J, Papassotiriou I, Giordano PC, Harteveld CL, Baudin-Creuza V, Old J (2008) Unstable and thalassemic alpha-chain hemoglobin variants: A cause of Hb H disease and thalassemia intermedia. Hemoglobin 32(4):327–349
12. Rother RP, Bell L, Hillmen P, Gladwin MT (2005) The clinical sequelae of intravascular hemolysis and extracellular plasma hemoglobin — A novel mechanism of human disease. Jama—J Am Med Assoc 293(13):1653–1662
13. Cho CW, Kim CW (2006) Toxicoproteomics in the study of aromatic hydrocarbon toxicity. Biotechnol Bioprocess Eng 11 (3):187–198
14. Vinagre AM, Collares EF (2007) Effect of 4-aminoantipyrine on gastric compliance and liquid emptying in rats. Braz J Med Biol Res 40(7):903–909
15. Sunderji SG, EI Badry A, Poore ER, Figueroa JP, Nathanielsz PW (1984) The effect of myometrial contractures on uterine blood flow in the pregnant sheep at 114 to 140 days' gestation measured by the 4-aminoantipyrine equilibrium diffusion technique. Am J Obstet Gynecol 149(4):408–412
16. EI Badry A, Figueroa JP, Poore ER, Sunderji S, Levine S, Mitchell MD, Nathanielsz PW (1984) Effect of fetal intravascular 4-aminoantipyrine infusions on myometrial activity (contractures)

at 125 to 143 days' gestation in the pregnant sheep. Am J Obstet Gynecol 150(5):474–479
17. Pierre SC, Schmidt R, Brenneis C, Michaelis M, Geisslinger G, Scholich K (2007) Inhibition of cyclooxygenases by dipyrone. Brit J Pharmacol 151(4):494–503
18. Wang YQ, Zhang HM, Wang RH (2008) Investigation of the interaction between colloidal TiO(2) and bovine hemoglobin using spectral methods. Colloid Surface B 65(2):190–196
19. Zhou J, Wu X, Gu X, Zhou L, Song K, Wei S, Feng Y, Shen J (2009) Spectroscopic studies on the interaction of hypocrellin A and hemoglobin. Spectrochim Acta A 72(1):151–155
20. Lakowicz JR, Weber G (1973) Quenching of fluorescence by oxygen. A probe for structural fluctuations in macromolecules. Biochemistry 12(21):4161–4170
21. Wang YQ, Zhang HM, Zhou QH, Xu HL (2009) A study of the binding of colloidal Fe_3O_4 with bovine hemoglobin using optical spectroscopy. Colloid Surface A 337(1–3):102–108
22. Liu XH, Xi PX, Chen FJ, Xu ZH, Zeng ZZ (2008) Spectroscopic studies on binding of 1-phenyl-3-(coumarin-6-yl)sulfonylurea to bovine serum albumin. J Photochem Photobiol B 92(2):98–102
23. Lu JQ, Jin F, Sun TQ, Zhou XW (2007) Multi-spectroscopic study on interaction of bovine serum albumin with lomefloxacin-copper (II) complex. Int J Biol Macromol 40(4):299–304
24. Xiang GH, Tong CL, Lin HZ (2007) Nitroaniline Isomers Interaction with Bovine Serum Albumin and Toxicological Implications. J Fluoresc 17(5):512–521
25. Wang YQ, Zhang HM, Zhang GC, Liu SX, Zhou QH, Fei ZH, Liu ZT (2007) Studies of the interaction between paraquat and bovine hemoglobin. Int J Biol Macromol 41(3):243–250
26. Wang YQ, Zhang HM, Zhang GC, Zhou QH, Fei ZH, Liu ZT, Li ZX (2008) Fluorescence spectroscopic investigation of the interaction between benzidine and bovine hemoglobin. J Mol Struct 886(1–3):77–84
27. Chen LH, Tianqing LQ (2008) Interaction behaviors between chitosan and hemoglobin. Int J Biol Macromol 42(5):441–446
28. Tao WS, Li W, Jiang YM (1995) Protein molecular basic. Higher Education Press, Beijing
29. Ran DH, Wu X, Zheng JH, Yang JH, Zhou HP, Zhang MF, Tang YJ (2007) Study on the interaction between florasulam and bovine serum albumin. J Fluoresc 17(6):721–726
30. Hu YJ, Liu Y, Wang JB, Xiao XH, Qu SS (2004) Study of the interaction between monoammonium glycyrrhizinate and bovine serum albumin. J Pharm Biomed Anal 36(4):915–919
31. Shen XC, Liou XY, Ye LP, Liang H, Wang ZY (2007) Spectroscopic studies on the interaction between human hemoglobin and US quantum dots. J Colloid Interf Sci 311(2):400–406